



HAL
open science

High-sensitivity CRDS absorption spectrum of ^{17}O enriched carbon dioxide near $1.74\ \mu\text{m}$

D. Mondelain, E.V. Karlovets, V.I. Perevalov, S.A. Tashkun, A. Campargue

► **To cite this version:**

D. Mondelain, E.V. Karlovets, V.I. Perevalov, S.A. Tashkun, A. Campargue. High-sensitivity CRDS absorption spectrum of ^{17}O enriched carbon dioxide near $1.74\ \mu\text{m}$. *Journal of Molecular Spectroscopy*, 2019, 362, pp.84-89. 10.1016/j.jms.2019.06.004 . hal-02271437

HAL Id: hal-02271437

<https://hal.science/hal-02271437>

Submitted on 25 Oct 2021

HAL is a multi-disciplinary open access archive for the deposit and dissemination of scientific research documents, whether they are published or not. The documents may come from teaching and research institutions in France or abroad, or from public or private research centers.

L'archive ouverte pluridisciplinaire **HAL**, est destinée au dépôt et à la diffusion de documents scientifiques de niveau recherche, publiés ou non, émanant des établissements d'enseignement et de recherche français ou étrangers, des laboratoires publics ou privés.



Distributed under a Creative Commons Attribution - NonCommercial 4.0 International License

High-sensitivity CRDS absorption spectrum of ^{17}O enriched carbon dioxide near $1.74\ \mu\text{m}$

D. Mondelain¹, E.V. Karlovets^{2,3}, V.I. Perevalov³, S.A. Tashkun³, A. Campargue^{1*}

¹ *Univ. Grenoble Alpes, CNRS, LIPhy, 38000 Grenoble, France*

² *Tomsk State University, Laboratory of Quantum Mechanics of Molecules and Radiative Processes, 36, Lenin Avenue, 634050, Tomsk, Russia*

³ *Laboratory of Theoretical Spectroscopy, V.E. Zuev Institute of Atmospheric Optics, Siberian Branch, Russian Academy of Sciences, 1, Academician Zuev Square, 634055 Tomsk, Russia*

Keywords: carbon dioxide; ^{17}O isotopologues; CRDS; spectroscopic database; HITRAN; CDSDB

Corresponding author: Alain Campargue (alain.campargue@univ-grenoble-alpes.fr)

Abstract

The room temperature absorption spectrum of ^{17}O enriched carbon dioxide is investigated by high sensitivity cavity ring down spectroscopy (CRDS) between 5695 and 5850 cm^{-1} . About 1100 lines are measured and assigned to 26 bands of the six ^{17}O containing carbon dioxide isotopologues: $^{16}\text{O}^{12}\text{C}^{17}\text{O}$, $^{16}\text{O}^{13}\text{C}^{17}\text{O}$, $^{17}\text{O}^{12}\text{C}^{18}\text{O}$, $^{17}\text{O}^{13}\text{C}^{18}\text{O}$, $^{12}\text{C}^{17}\text{O}_2$ and $^{13}\text{C}^{17}\text{O}_2$. The set of observed lines are rovibrationally assigned on the basis of the predictions of the effective Hamiltonian (EH) model. The observed bands belong to the $\Delta P=8$ and 9 series of transitions where $P=2V_1+V_2+3V_3$ is the polyad number (V_i being the vibrational quantum numbers). They consist in 12 previously unobserved bands and 14 already-known bands, for which additional high J lines are assigned. Bands of the $^{12}\text{C}^{17}\text{O}_2$ and $^{13}\text{C}^{17}\text{O}_2$ isotopologues (two for each) are observed for the first time in this spectral interval. The accurate spectroscopic parameters of the upper vibrational levels are determined from a band-by-band fit of the line positions (typical *rms* deviations are less than 0.001 cm^{-1}). The comparison to the most recent carbon dioxide spectroscopic databases is presented. The reported data will be used to improve the modeling of the line positions of ^{17}O containing carbon dioxide isotopologues.

1. Introduction

The absorption spectrum of natural carbon dioxide shows a spectral interval of very weak absorption near $1.74 \mu\text{m}$ [1]. In particular, in the $5700\text{-}5775 \text{ cm}^{-1}$ interval, all the transitions of natural CO_2 have an intensity smaller than $10^{-28} \text{ cm/molecule}$ which makes this “transparency window” very interesting to sound the deep atmosphere and the surface of Venus [2]. It is well known that transparency windows are spectral regions where lines of minor isotopologues may show up with relative intensities much larger than the isotopic abundance [3-5]. This is due to the isotopic shift of the vibrational bands or to the difference in symmetry of the isotopologues which leads to different selection rules (for instance in $^{12}\text{C}^{16}\text{O}_2$ and $^{16}\text{O}^{12}\text{C}^{18}\text{O}$ [3]).

In the recent year, we have dedicated three studies to detailed analysis of the absorption of the twelve stable CO_2 isotopologues in $1.74 \mu\text{m}$ transparency window by high sensitivity cavity ring down spectroscopy (CRDS). These previous works were dedicated to natural [1], ^{18}O enriched [6] and ^{13}C carbon dioxide [7]. In the present work, a ^{17}O enriched sample is used to characterize the transitions of the six ^{17}O enriched species: $^{16}\text{O}^{12}\text{C}^{17}\text{O}$ (627 in HITRAN notation [8]), $^{16}\text{O}^{13}\text{C}^{17}\text{O}$ (637), $^{17}\text{O}^{12}\text{C}^{18}\text{O}$ (728), $^{17}\text{O}^{13}\text{C}^{18}\text{O}$ (738), $^{12}\text{C}^{17}\text{O}_2$ (727) and $^{13}\text{C}^{17}\text{O}_2$ (737).

The description of the experimental details and line list construction are given in Section 2. The rovibrational assignments and band-by-band analysis are presented in Section 3 while the present observations are compared to various spectroscopic databases of carbon dioxide in Section 4.

2. Experiment details

The present CRDS spectra of ^{17}O enriched carbon dioxide were recorded between 5695 and 5850 cm^{-1} at room temperature (about 294 K) with a total pressure of 7.5 Torr . The setup description has been presented in Ref. [1]. Eight distributed feedback (DFB) laser diodes were used as light sources. The DFB typical tuning range was about 20 cm^{-1} by temperature increase from -5°C to 55°C allowing the coverage of the $5694\text{-}5851 \text{ cm}^{-1}$ range except for a few spectral gaps: $5714.74\text{-}5725.33$, $5774.96\text{-}5781.54$, $5793.20\text{-}5794.95$, $5806.58\text{-}5810.49 \text{ cm}^{-1}$. Temperature and pressure were measured with a temperature sensor (TSic 501, IST-AG, 0.1 K accuracy) fixed on the cell surface and a 10 Torr pressure gauge (Baratron, model 122BA, accuracy 0.15% of reading), respectively.

The ^{17}O -enriched gas sample was obtained by injecting carbon dioxide in natural isotopic abundance in a tank containing a droplet of water highly enriched in ^{17}O (from

Sigma Aldrich). According to the certificate of analysis obtained by mass spectrometry, the ^{17}O enriched water sample used has the following stated relative abundance of the oxygen atoms: ^{16}O : 28%, ^{17}O : 70% and ^{18}O : 2%. (In fact, the real ^{17}O enrichment of water in the tank is probably lower as a consequence of the exchange with water molecules adsorbed on the walls of the cell). An almost complete isotopic exchanges of oxygen atoms between water vapour and carbon dioxide is achieved after a few hours. The tank temperature was then decreased below 273 K to condensate water and keep only CO_2 in the gas phase. The optical cell was then filled with the purified ^{17}O -enriched CO_2 gas. This latter procedure of purification was applied for each filling of the CRDS cell. Despite, this purification procedure, water vapor is still present in the CO_2 gas sample at a partial pressure between 0.1 and 1 Torr. The water contribution to the total gas pressure combined with uncertainties on the relative isotopic abundances prevented absolute line intensities to be determined accurately. The approximate values of the line intensities included in the Supplementary Material were nevertheless of importance in the assignment process (see below).

A section of the spectrum showing transitions of the 628, 728 and 627 isotopologues was recorded just after the filling of the cell and 72 hours later. The partial pressure of these three isotopologues was derived from the fitted area of the transitions using a Voigt profile and HITRAN2016 values of the line intensities [8]. Assuming a statistical mixing of the different CO_2 isotopologues and a standard isotopic abundance for the carbon atoms (0.9842 for ^{12}C), the following isotopic abundances of the (^{16}O , ^{17}O , ^{18}O) atoms were obtained: (0.462, 0.306, 0.247) and (0.439, 0.322, 0.212) just after the filling and 72 hours later, respectively. (Note that the sum differs from 1.0 by a few %, probably due to experimental uncertainties). The small evolution of the isotopic composition results from isotopic exchanges between the gaseous phase and the walls of the cell which was previously used to record spectra of the ^{17}O -enriched water vapour sample [9].

Table 1. Relative abundances, number of bands and transitions analyzed for the six ^{17}O -containing carbon dioxide isotopologues in 5695-5850 cm^{-1} region.

Isotopologue	Abundance (%)	Number of transitions	Number of bands ^a
$^{16}\text{O}^{12}\text{C}^{17}\text{O}$	28.0	265	6(4)
$^{16}\text{O}^{13}\text{C}^{17}\text{O}$	0.28	152	4(1)
$^{17}\text{O}^{12}\text{C}^{18}\text{O}$	15.0	563	10(2)
$^{12}\text{C}^{17}\text{O}_2$	9.3	40	2(2)
$^{17}\text{O}^{13}\text{C}^{18}\text{O}$	0.15	54	2(1)
$^{13}\text{C}^{17}\text{O}_2$	0.09	26	2(2)
Total		1100	26(12)

Note

^aThe number of bands newly observed in this work is given in parenthesis.

From the measured abundances values, the isotopic abundance of the twelve stable CO₂ isotopologues was calculated assuming a statistical distribution. The obtained values of the relative abundances of the six ¹⁷O-containing carbon dioxide isotopologues are given in **Table 1**.

The typical minimal detectable absorption coefficient was measured to be in the 1-5×10⁻¹¹ cm⁻¹ range depending of the wavenumber. A commercial Fizeau-type wavelength meter (HighFinesse WSU7-IR, 5 MHz resolution, 20 MHz accuracy over 10 hours) was used for calibration of the frequency values. This calibration was then refined using accurate CO₂ line positions provided by the HITRAN2016 database leading to an uncertainty on the order of 0.001 cm⁻¹ on the line positions.

The experimental list limited to the rovibrational transitions of the six ¹⁷O containing carbon dioxide isotopologues was constructed. The line centers and intensities were determined using a homemade interactive least squares multi-line fitting program assuming a Voigt profile. **Fig. 1** illustrates the quality of the simulation of the CRDS spectrum. In most cases, the Gaussian HWHM was fixed to the theoretical value of the Doppler width. The multi-line fit provides then integrated line absorption coefficient, line center, Lorentzian width and the corresponding local baseline (assumed to be a linear function of the wavenumber). We estimate the accuracy of line positions to be about 1×10⁻³ cm⁻¹ and the combined standard uncertainty of measured line intensities (including the error on the pressure value) to be better than 3% for isolated not weak lines.

The line intensity, S_{ν_0} (cm/molecule), of a rovibrational transition centered at ν_0 , was obtained from the integrated absorption coefficient, A_{ν_0} (cm⁻²):

$$A_{\nu_0}(T) = \int_{line} \alpha_{\nu} d\nu = S_{\nu_0}(T)N \quad (1)$$

where:

- ν is the wavenumber in cm⁻¹,
- α_{ν} is the absorption coefficient in cm⁻¹ obtained from the cavity ring down time, τ (in s): $\alpha = \frac{1}{c} \left(\frac{1}{\tau} - \frac{1}{\tau_0} \right)$ where c is the light velocity and τ_0 is the ring-down time of the empty cavity
- N is the molecular concentration in molecule/cm³ obtained from the measured pressure (P) and temperature (T) values: $P = NkT$ (k is the Boltzmann constant).

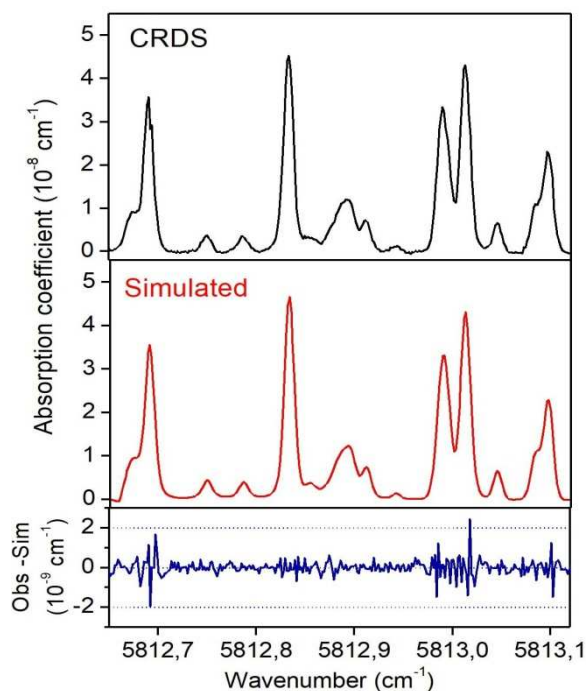


Fig. 1.

Fragment of the observed (top panel) and simulated (middle panel) CRDS spectrum of ^{17}O enriched carbon dioxide near 5812 cm^{-1} at 7.5 Torr. The residuals between observed and simulated spectra are given in the bottom panel.

3. Spectrum analysis

3.1. Rovibrational assignments

A total of 1100 lines belonging to 26 bands of $^{16}\text{O}^{12}\text{C}^{17}\text{O}$, $^{16}\text{O}^{13}\text{C}^{17}\text{O}$, $^{17}\text{O}^{12}\text{C}^{18}\text{O}$, $^{12}\text{C}^{17}\text{O}_2$, $^{17}\text{O}^{13}\text{C}^{18}\text{O}$ and $^{13}\text{C}^{17}\text{O}_2$ were rovibrationally assigned by comparison to spectra calculated using an effective operator approach. The effective Hamiltonian (EH) is a polyad model [10], each polyad of interacting vibrational states resulting from the approximate relations between the harmonic frequencies $\omega_1 \approx 2\omega_2$ and $\omega_3 \approx 3\omega_2$ is labeled by an integer $P = 2V_1 + V_2 + 3V_3$ (where V_i are the vibrational quantum numbers). All assigned rovibrational bands (eight cold and eighteen hot bands) correspond to $\Delta P = 8$ and 9 series of transitions. The calculated spectra used the EH and effective dipole moment (EDM) parameters derived for each isotopologue in the following references: Refs. [5,11] for $^{16}\text{O}^{12}\text{C}^{17}\text{O}$ and $^{12}\text{C}^{17}\text{O}_2$; Ref. [5] for $^{16}\text{O}^{13}\text{C}^{17}\text{O}$, $^{17}\text{O}^{12}\text{C}^{18}\text{O}$ and $^{17}\text{O}^{13}\text{C}^{18}\text{O}$, Refs. [12,13] for $^{13}\text{C}^{17}\text{O}_2$. In the case of the last isotopologue for the line intensities predictions, the EDM parameters of the principal isotopologue were used. In this work, the $^{12}\text{C}^{16}\text{O}_2$, $^{13}\text{C}^{16}\text{O}_2$, $^{16}\text{O}^{12}\text{C}^{18}\text{O}$, $^{16}\text{O}^{13}\text{C}^{18}\text{O}$, $^{12}\text{C}^{18}\text{O}_2$ and $^{13}\text{C}^{18}\text{O}_2$ are not considered because most observations for these isotopologues were obtained by our CRDS studies in the same spectral region [1,6,7].

Table 1 includes the numbers of transitions and bands assigned in the present work to

those previously observed in the studied region. Previous observations consist mainly in the CRDS data obtained in Refs. [1,6,7]. Note that 12 of the 26 assigned bands are newly reported. Additional *J* lines were assigned for the 14 already-known bands. The observed hot bands access upper states of the *P*= 9-12 polyads. The most excited upper level detected in this study is the 41115 level near 7716.20 cm^{-1} observed through the 41115-11102 hot band at 5830.76 cm^{-1} .

As an illustration of the difficulties of the assignments, **Fig. 2** shows a sample of a 1 cm^{-1} spectral interval around 5751.4 cm^{-1} where transitions of eight CO₂ isotopologues are observed.

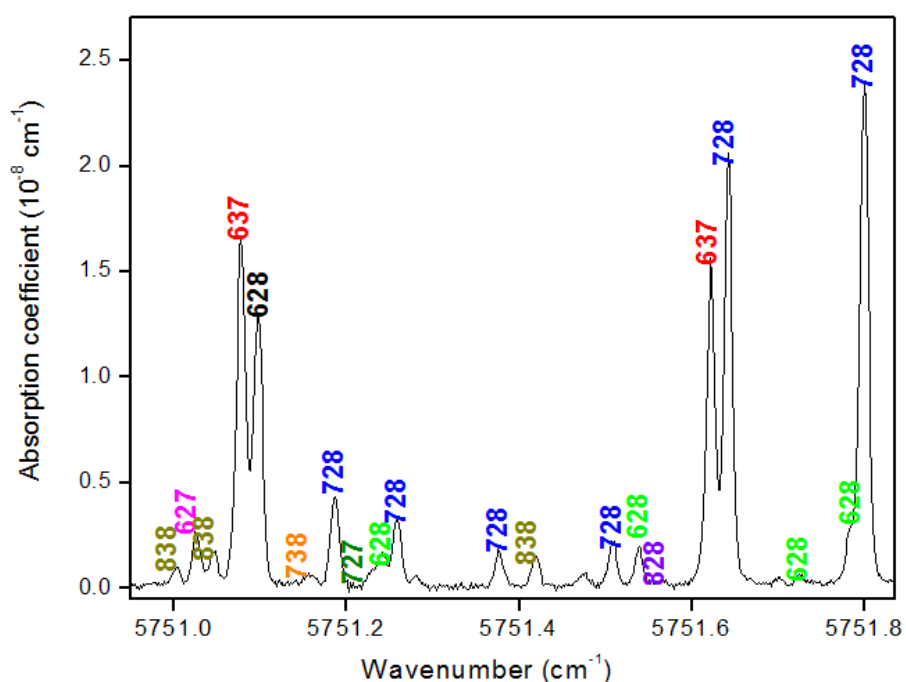


Fig. 2.

CRDS spectrum of ¹⁷O enriched carbon dioxide recorded at 7.5 Torr near 5751.4 cm^{-1} . Transitions due to eight CO₂ isotopologues are marked: 628 (¹⁶O¹²C¹⁸O), 627 (¹⁶O¹²C¹⁷O), 637 (¹⁶O¹³C¹⁷O), 828 (¹²C¹⁸O₂), 728 (¹⁷O¹²C¹⁸O), 727 (¹²C¹⁷O₂), 838 (¹³C¹⁸O₂) and 738 (¹⁷O¹³C¹⁸O).

Fig. 3 shows an overview comparison between the present observations and the predicted spectra for the six carbon dioxide isotopologues. The line intensities of all CO₂ species are given at 296K and correspond to the isotopologue abundance values given in **Table 1**. The smallest intensity values are on the order of $2 \times 10^{-29}\text{ cm/molecule}$. The complete line list including the isotopologue identification, rovibrational assignments and the experimental and calculated values of the line positions and intensities is provided as Supplementary Material.

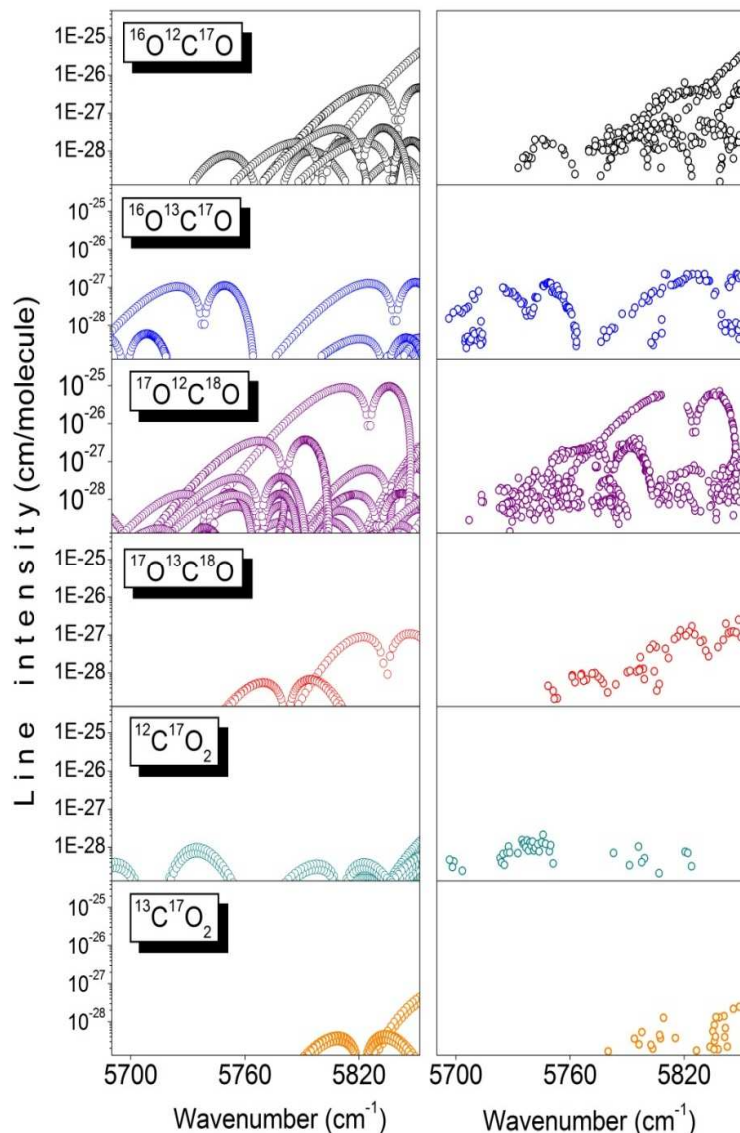


Fig. 3.

Overview comparison between the CRDS observations (right panels) in the 5695-5850 cm^{-1} spectral region and the predictions (left panels) within the framework of the method of effective operators for the $^{16}\text{O}^{12}\text{C}^{17}\text{O}$, $^{16}\text{O}^{13}\text{C}^{17}\text{O}$, $^{17}\text{O}^{12}\text{C}^{18}\text{O}$, $^{12}\text{C}^{17}\text{O}_2$, $^{17}\text{O}^{13}\text{C}^{18}\text{O}$ and $^{13}\text{C}^{17}\text{O}_2$ isotopologues.

The $^{16}\text{O}^{13}\text{C}^{17}\text{O}$, $^{17}\text{O}^{13}\text{C}^{18}\text{O}$ and $^{13}\text{C}^{17}\text{O}_2$ isotopologues have a relative abundance smaller than 0.3% in our sample (see **Table 1**). Among the four $^{16}\text{O}^{13}\text{C}^{17}\text{O}$ bands (152 lines), only the 11122-01101 hot band is newly reported, the other bands having been reported in the previous CRDS studies [1,6,7]. In the case of the two $^{17}\text{O}^{13}\text{C}^{18}\text{O}$ bands, the 31114-01101 hot band is newly detected while the 30014-00001 cold band was observed with the ^{18}O enriched sample [6]. In spite of a relative concentration of only 0.09%, two $^{13}\text{C}^{17}\text{O}_2$ bands are identified. All these bands correspond to the $\Delta P=9$ series of transitions and are very weak. Overall, 265 transitions of $^{16}\text{O}^{12}\text{C}^{17}\text{O}$ belonging to 6 bands were assigned. Previous observations in the region are limited to two bands detected in the CRDS spectrum of natural and ^{18}O enriched

carbon dioxide [1,6]. Only two bands (40015-10001 and 41115-11102) of the ten $^{17}\text{O}^{12}\text{C}^{18}\text{O}$ bands [6] are observed for the first time.

Fig 4 shows an overview position comparison to the EH predictions for the six ^{17}O isotopologues. The overall agreement of the EH predicted and measured line positions is good. Most of the differences are within $\pm 0.005\text{ cm}^{-1}$. Nevertheless, deviations about 0.01 cm^{-1} are noted for four bands: 41104-00001 of $^{16}\text{O}^{12}\text{C}^{17}\text{O}$, 32214-02201 of $^{17}\text{O}^{12}\text{C}^{18}\text{O}$, 41104-00001 and 40015-10001 of $^{12}\text{C}^{17}\text{O}_2$. Consequently, the set of new observations for the above CO_2 isotopologues will be valuable to improve the corresponding EH parameters.

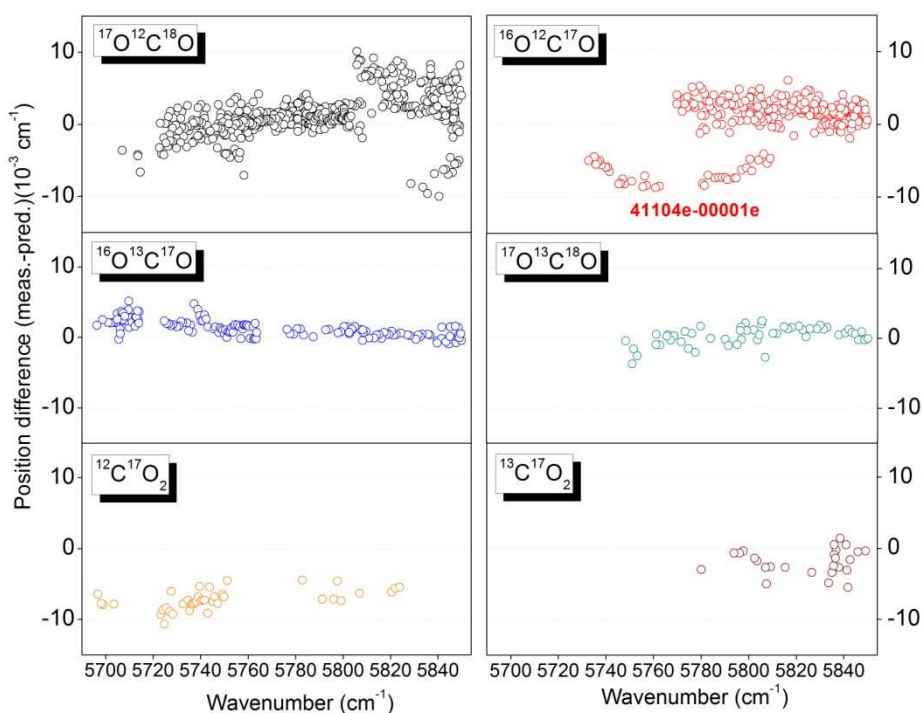


Fig. 4.

Differences between the line positions of the $^{16}\text{O}^{12}\text{C}^{17}\text{O}$, $^{16}\text{O}^{13}\text{C}^{17}\text{O}$, $^{17}\text{O}^{12}\text{C}^{18}\text{O}$, $^{12}\text{C}^{17}\text{O}_2$, $^{17}\text{O}^{13}\text{C}^{18}\text{O}$ and $^{13}\text{C}^{17}\text{O}_2$ lines measured in the $5695\text{-}5850\text{ cm}^{-1}$ region and values calculated by the method of effective operators.

3.2. Band-by-band analysis of the line positions

The rotational analysis was performed using the usual expression for the rotational energy of an isolated vibrational state:

$$F_v(J) = G_v + B_v J(J+1) - D_v J^2(J+1)^2 + H_v J^3(J+1)^3 \quad (1)$$

where G_v is the vibrational term value, B_v is the rotational constant, D_v and H_v are the centrifugal distortion constants, J is the angular momentum quantum number.

The band-by-band analysis allowed for deriving accurate spectroscopic parameters of 26 bands from the fits of the measured line positions. Note that most of the absorption lines of

our experimental list belong to hot bands. As the e and f sub-bands may be perturbed in a different way, different set of spectroscopic parameters were fitted for the e and f levels. **Table 2** lists, for each isotopologue, the obtained constants in increasing order of the band centers. The lower state constants were constrained to the values reported in Ref. [14] ($^{17}\text{O}^{13}\text{C}^{18}\text{O}$ and $^{13}\text{C}^{17}\text{O}_2$), Ref. [15] ($^{17}\text{O}^{12}\text{C}^{18}\text{O}$ and $^{12}\text{C}^{17}\text{O}_2$) and Ref. [16] ($^{16}\text{O}^{12}\text{C}^{17}\text{O}$ and $^{16}\text{O}^{13}\text{C}^{17}\text{O}$). The rotational and centrifugal distortion constants for 11102 e and 11102 f lower states were determined from the present band-by-band fit (See notes in **Table 2**). When possible, the input dataset used in the fits was extended in two ways: by completing with CRDS measurements from Refs. [1,6,7] and by adding CRDS line positions measured above 5850 cm^{-1} with a sample with a strong ^{18}O enrichment and a significant ^{17}O enrichment [5]. The detailed results of the band-by-band fit are provided as Supplementary Material. After exclusion of some outliers, the typical *rms* of the (*obs.-calc.*) deviations is generally better than $1 \times 10^{-3} \text{ cm}^{-1}$ which is consistent with our estimated uncertainty on the line positions. The line positions excluded from the fits or taken from other sources are indicated in the Supplementary Material.

4. Comparison to databases and concluding remarks

An overview of the deviations between the measured positions and the values of NASA Ames [17] and HITRAN2016 [8] for $^{16}\text{O}^{12}\text{C}^{17}\text{O}$, $^{16}\text{O}^{13}\text{C}^{17}\text{O}$ and $^{17}\text{O}^{12}\text{C}^{18}\text{O}$ is presented in **Fig. 5**. Due to the HITRAN intensity cut-off, only part of the observations can be compared to HITRAN data. A good agreement with HITRAN2016 is obtained for the $^{16}\text{O}^{12}\text{C}^{17}\text{O}$ and $^{16}\text{O}^{13}\text{C}^{17}\text{O}$ isotopologues (differences within $\pm 0.002 \text{ cm}^{-1}$). The source of the HITRAN2016 line positions is the CDS-296 line list of Ref. [18] based on the global modeling of the line positions (and intensities) using the effective operators approach [10,19-21]. Note that the positions of the recently released updated version of CDS-296 [22] are very close to those of the previous version [18]. The variational NASA Ames line positions based on an empirically refined potential energy surface deviate from the CRDS values by differences up to 0.04 cm^{-1} . As mentioned above, our line intensities are not sufficiently accurate for comparisons as they are affected by important uncertainties on the relative isotopic abundance in our sample and by the presence of a significant amount of water vapor in the used sample.

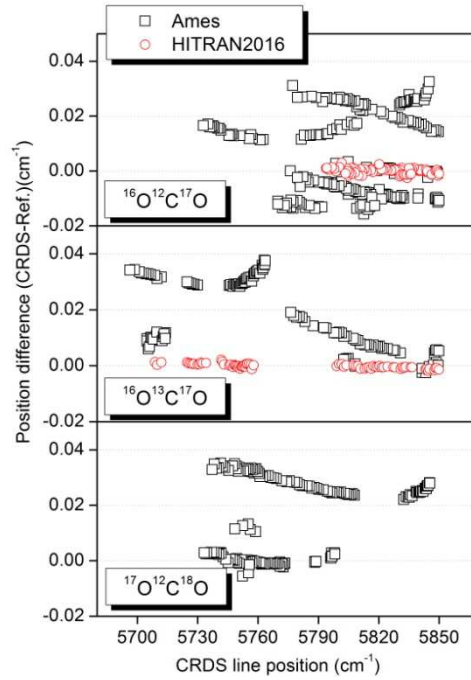


Fig. 5

Differences between the measured line positions and the values from NASA Ames line list [17] (black symbols) and HITRAN2016 [8] (red symbols) for the $^{16}\text{O}^{12}\text{C}^{17}\text{O}$, $^{16}\text{O}^{13}\text{C}^{17}\text{O}$ and $^{17}\text{O}^{12}\text{C}^{18}\text{O}$ isotopologues in the 5695-5850 cm^{-1} region.

This paper is the fourth and last one of a series devoted to the analysis of the absorption spectrum of carbon dioxide in the 1.74 μm transparency window [1,6,7]. As a result of the weakness of the transitions located in the considered 5690-5850 cm^{-1} region, previous observations by Fourier transform spectroscopy were very scarce. The CRDS measurements have allowed for critical validation tests for the most recent spectroscopic databases. In particular, some issues concerning the present status of the HITRAN2016 line list have been revealed and identified as due to the mixing of the CDS-296 [18] and *ab initio* line intensities in the HITRAN list [1,5,7]. In a number of cases, *ab initio* intensities should have been preferred to the CDS-296 intensities. This is the case of the intensities of weak perturbed $\Delta P=9$ perpendicular bands (for instance, 4110*i*-00001, *i*= 1-5) which were poorly predicted in the CDS-296 [18] (see Refs. [1,6,7]). Nevertheless, CDS-296 line positions show an overall good agreement with the observations for all the isotopologues. Some significant deviations on the order of 0.01 cm^{-1} indicate that the modeling of the carbon dioxide absorption in the region could be further improved on the basis of the present CRDS study. Note, that using new CRDS measurements [1,5,7] the problem of the line intensities of the weak perpendicular bands of the $\Delta P=9$ series has been solved in the recent updated version of the CDS-296 [22]. The new sets of EDM parameters reproduce the observed line intensities within their measurement uncertainties.

Acknowledgements

This work was performed in the frame of the Laboratoire International Associé SAMIA supported by CNRS (France) and UGA. This work was performed in the frame of the Mendeleev Foundation of Tomsk State University.

References

1. P. Čermák, E.V. Karlovets, D. Mondelain, S. Kassi, V.I. Perevalov, A. Campargue, J. Quant. Spectrosc. Radiat. Transf. 207(2018) 95–103.
2. B. Bézard B, C. de Bergh. J. Geophys. Res. 112(2007) E04S07.
3. E.V. Karlovets, A. Campargue, D. Mondelain, S. Béguier, S. Kassi, S.A.Tashkun, V.I. Perevalov, J. Quant. Spectrosc. Radiat. Transf. 130 (2013) 116–33.
4. E.V. Karlovets, A. Campargue, D. Mondelain, S. Kassi, S.A.Tashkun, V.I. Perevalov, J. Quant. Spectrosc. Radiat. Transf. 136 (2014) 71–88.
5. E V. Karlovets, A.Campargue, D. Mondelain, S. Kassi, S.A.Tashkun, V.I. Perevalov, J. Quant. Spectrosc. Radiat. Transf. 136 (2014) 89–107.
6. E.V. Karlovets, P. Čermák, D. Mondelain, S. Kassi, A. Campargue, S.A. Tashkun, V.I. Perevalov, J. Quant. Spectrosc. Radiat. Transf. 217 (2018) 73-85.
7. E.V. Karlovets, A.D. Sidorenko, P. Čermák, D. Mondelain, S. Kassi, V.I. Perevalov, A.Campargue, J. Mol. Spectrosc.354 (2018) 54-59.
8. I.E. Gordon, L.S. Rothman, C. Hill, R.V. Kochanov, Y. Tan, P.F. Bernath, et al., J. Quant. Spectrosc. Radiat. Transf. 203 (2017) 3–69.
9. S.N. Mikhailenko, D. Mondelain, E.V. Karlovets, S. Kassi, A. Campargue, J. Quant. Spectrosc. Radiat. Transf. 222-223 (2019) 229-235.
10. J.L. Teffo, O.N. Sulakshina, V.I. Perevalov, J. Mol. Spectrosc. 156 (1992) 48–64.
11. Y.G. Borkov, D. Jacquemart, O.M. Lyulin, S.A. Tashkun, V.I. Perevalov, J. Quant. Spectrosc. Radiat. Transf. 137 (2014) 57–76.
12. S.A. Tashkun. Proceedings of the XVII symposium on high resolution molecular spectroscopy, Zelenogorsk, St.Petersburg region, Russia. (2012) 67.
13. B.V. Perevalov, A. Campargue, B. Gao, S. Kassi, S.A. Tashkun, V.I. Perevalov, J. Mol. Spectrosc. 252 (2008) 190-197.
14. J.L. Teffo, C. Claveau, A. Valentin, J. Quant. Spectrosc. Radiat. Transf. 59(1998) 151-164.
15. C. Claveau, J.L. Teffo, D. Hurtmans, A. Valentin, J. Mol. Spectrosc. 189 (1998) 153–195.
16. L.S. Rothman, R.L. Hawkins, R.B. Wattson, R.R. Gamache, J. Quant. Spectrosc. Radiat. Transf. 48 (1992) 537–566.
17. X. Huang, D.W. Schwenke, R.S. Freedman, T.J. Lee, J. Quant. Spectrosc. Radiat. Transf. 203 (2017) 224–241.
18. S.A. Tashkun, V.I. Perevalov, R.R. Gamache, J. Lamouroux, J. Quant. Spectrosc. Radiat. Transf. 152 (2015) 45–73.
19. V.I. Perevalov, E.I. Lobodenko, O.M. Lyulin, J.L. Teffo, J. Mol. Spectrosc. 171(1995) 435–452.
20. J.L. Teffo, O.M. Lyulin, V.I. Perevalov, E.I. Lobodenko, J. Mol.Spectrosc. 187 (1998) 28–41.
21. S.A. Tashkun, V.I. Perevalov, J.L. Teffo, V.G. Tyuterev, J. Quant. Spectrosc. Radiat. Transf. 62 (1999) 571-598.
22. S.A. Tashkun, V.I. Perevalov, R.R. Gamache, J. Lamouroux, J. Quant. Spectrosc. Radiat. Transf. 228 (2019) 124–131.

Table 2.

Spectroscopic constants (in cm^{-1}) of the bands of the ^{17}O isotopologues of CO_2 obtained from the analysis of the CRDS spectrum recorded in the 5695–5850 cm^{-1} region with a ^{17}O enriched sample.

ΔP^a	Band	ΔG_v^b	G_v	B_v	$D_v \times 10^7$	$H_v \times 10^{12}$	rms^c	$N_{TW}/N_{fit}/N_{all}^d$	J_{max}^e P/Q/R	Added lines ^f
$^{16}\text{O}^{12}\text{C}^{17}\text{O}$										
9	41104e-00001e	5773.27623(36)	5773.27623(36)	0.37826779(70)	1.5830(26)		0.75	37/37/37	P52/R48	
8	12222e-02201e 12222e-02201f	5800.90001(42)	7130.74301(42)	0.3744661(15)	1.244(11)		0.82	14/13/14 3/3/3	P33/R37 Q4	
	12222f-02201f 12222f-02201e	5800.90106(44)	7130.74406(44)	0.3744630(13)	1.3188(56)		0.98	22/19/22 1/1/1	P33/R46 Q6	
8	20023e-10002e	5821.53104(32)	7093.81767(32)	0.37357280(80)	1.6688(35)		0.90	45/40/45	P45/R48	
8	20022e-10001e	5836.87138(43)	7212.89885(43)	0.3721231(20)	1.223(14)		0.77	20/18/20	P38/R19	
8	11122e-01101e 11122e-01101f	5840.57420(16)	6505.30334(16)	0.37327703(35)	1.3786(12)		0.79	44/69/72 6/6/6	P59/R12 Q16	[1]
	11122f-01101f 11122f-01101e	5840.57362(15)	6505.30276(15)	0.37411382(34)	1.4591(13)		0.75	46/67/73 4/4/4	P57/R13 Q18	[1]
8	10022e-00001e	5885.32087(10)	5885.32087(10)	0.37292426(15)	1.47643(41)		0.70	23/158/159	P67/R52	[1,5,6]
$^{16}\text{O}^{13}\text{C}^{17}\text{O}$										
8	11122e-01101e 11122f-01101f	5697.1953(11) 5697.1904(21)	6342.9393(11) 6342.9344(21)	0.3736931(57) 0.374676(12)	1.340(59) 1.69(13)		0.74 0.92	14/14/14 11/9/11	R27 R26	
	8	10022e-00001e	5738.066735(99)	5738.066735(99)	0.37355961(22)	1.46104(93)		0.76	65/175/181	P43/R53
8	11121e-01101e 11121f-01101f	5834.07129(49) 5834.07226(58)	6479.81529(49) 6479.81626(58)	0.3728569(15) 0.3736490(17)	1.1035(77) 1.08451(87)		0.95 0.89	9/17/22 6/15/19	P46/R25 P45/R25	[7]
	8	10021e-00001e	5838.933866(82)	5838.933866(82)	0.37246068(20)	1.08286(72)		0.52	47/121/125	P57/R17
$^{17}\text{O}^{12}\text{C}^{18}\text{O}$										
9	12222e-02201e	5741.81328(39)	7061.63204(39)	0.3528606(14)	1.2668(97)		0.94	17/32/33	P40/R29	[6]
9	12222f-02201f	5741.81329(48)	7061.63205(48)	0.3528604(19)	1.246(15)		0.99	14/22/23	P38/R26	[6]
9	40015e-10001e	5768.06206(54)	7123.71628(54)	0.3553612(23)	1.857(17)		0.91	19/19/19	P34/R34	
8	20022e-10001e	5768.23615(32)	7123.89037(32)	0.35100394(97)	1.0087(56)		0.88	36/48/50	P43/R36	[6]
8	20023e-10002e	5768.30091(18)	7012.89504(18)	0.35166360(56)	1.4915(33)		0.76	56/84/88	P43/R40	[6]
9	11122e-01101e	5781.14105(11)	6440.84270(11)	0.35174247(20)	1.22745(68)		0.78	89/150/152	P64/R51	[6]

	11122e-01101f							4/4/4	Q5	
	11122f-01101f 11122f-01101e	5781.14075(11)	6440.84240(11)	0.35244992(23)	1.28442(89)		0.70	88/151/155 5/5/5	P57/R52 Q9	[6]
9	10022e-00001e	5825.331691(92)	5825.331691(92)	0.35127482(19)	1.28041(96)	0.127(13)	0.60	99/211/213	P75/R74	[6]
9	41115e-11102e ^b	5830.76249(41)	7716.20049 ^g	0.354981(16)	1.68(26)		0.54	19/19/19	P19/R25	
	41115f-11102f ^b	5830.76295(41)	7716.20240 ^g	0.356595(12)	1.72(11)		0.60	21/21/21	P32/R26	
9	32214e-02201e 32214e-02201f	5837.22572(30)	7157.04448(30)	0.3559936(13)	1.1187(98)		0.91	29/40/45 2/2/2	P41/R19 Q12	[6]
	32214f-02201f 32214f-02201e	5837.22627(27)	7157.04503(27)	0.3559962(11)	1.4027(83)		0.83	29/46/46 2/2/2	P39/R20 Q12	[6]
9	40015e-10002e	5879.12319(37)	7123.71732(37)	0.35535552(62)	1.8291(23)		0.76	13/25/25	P56	[6]
9	31114e-01101e	5887.52752(20)	6547.22917(20)	0.35479050(72)	1.4831(55)	2.05(11)	0.65	8/65/67	P59/R42	[5,6]
	31114f-01101f	5887.52781(14)	6547.22946(14)	0.35603267(43)	1.6188(25)	0.392(38)	0.55	13/78/86	P69/R44	[5,6]
¹² C ¹⁷ O ₂										
9	41104e-00001e	5714.58857(47)	5714.58857(47)	0.36672856(83)	1.4437(30)		0.84	P24/R51	31/28/31	
9	40015e-10001e	5810.60894(98)	7175.54931(98)	0.3659313(43)	2.010(33)		0.89	P35/R18	9/9/9	
¹⁷ O ¹³ C ¹⁸ O										
9	31114e-01101e	5781.93556(90)	6422.49940(90)	0.3553901(30)	1.485(19)		0.92	P39/R25	8/8/8	
	31114f-01101f	5781.93561(53)	6422.49945(53)	0.3568796(17)	1.6116(92)		0.93	P44/R36	17/17/17	
9	30014e-00001e	5834.30416(19)	5834.30416(19)	0.35570777(61)	1.7164(28)		0.70	P48/R24	27/44/44	[6]
¹³ C ¹⁷ O ₂										
9	31114e-01101e	5821.37859(12)	6464.38072(12)	0.3658276(51)	1.627(48)		0.82	P30/R29	8/8/8	
	31114f-01101f	5821.37794(68)	6464.38006(68)	0.3674389(14)	1.7099(47)		0.82	P53/R29	12/12/12	
9	30014e-00001e	5872.1412(41)	5872.1412(41)	0.3661848(60)	1.861(20)		0.46	P46	6/6/6	

Notes

The confidence interval (1SD) is in the units of the last quoted digit.

^a $\Delta P = P' - P''$ ($P = 2V_1 + V_2 + 3V_3$ is the polyad number).

^b $\Delta G_v = G_v' - G_v''$ is the band center.

^c Root Mean Square of the (Obs.-Calc.) differences of the line position values (10^{-3} cm^{-1}).

^d N_{TW} is number of lines measured in this work; N_{fit} is number of lines included in the fit, N_{all} is the total number of measured line positions available for the considered band (including literature data [1,5-7]).

^e Observed branch with the maximum value of the total angular momentum quantum number.

^f Literature source used to complete the input dataset of the considered band.

^g The upper vibrational term value, G_v , was obtained by adding ΔG_v to the EH value of the lower state vibrational term: $G_{low} = 1885.43800$ and $1885.43945 \text{ cm}^{-1}$ for 11102e and 11102f, respectively.

^h The lower state rotational and centrifugal distortion constants were determined from the present band-by-band fit (11102e: $B_v = 0.357191(17)$ and $D_v = 1.258(31) \times 10^{-7} \text{ cm}^{-1}$; 11102f: $B_v = 0.357892(11)$ and $D_v = 1.243(93) \times 10^{-7} \text{ cm}^{-1}$).

